

Adiabatic Ionization Energies, Bond Disruption Enthalpies, and Solvation Free Energies for Gas-Phase Metallocenes and Metallocenium Ions

Matthew F. Ryan, John R. Eyler, and David E. Richardson*

Contribution from the Department of Chemistry, University of Florida, Gainesville, Florida 32611-2046. Received March 13, 1992

Abstract: Free energies of ionization for Cp_2V , Cp_2Mn , Cp_2Fe , Cp_2Ni , Cp_2Ru , Cp_2Os ($Cp = \eta^5$ -cyclopentadienyl), and a series of ferrocene derivatives have been determined through gas-phase electron-transfer equilibrium (ETE) reactions by using Fourier transform ion cyclotron resonance mass spectrometry. Temperature dependence studies involving ETE of ferrocene with *N,N*-diethyltoluidine lead to a value of the enthalpy of ionization, ΔH_i° , for ferrocene of 6.82 ± 0.08 eV. Experimental and statistical mechanical analyses indicate that the one-electron oxidation of ferrocene is accompanied by a positive entropy of ionization, ΔS_i° , most of which is associated with changes in the electronic and vibrational contributions to the partition functions of ferrocene and the ferrocenium ion. Ionization energies of alkylferrocene derivatives are correlated with alkyl Taft parameters. Thermochemical cycles are used to derive estimates of average homolytic and heterolytic bond disruption enthalpies (ΔH_{hom}° and ΔH_{het}°) for selected metallocenium ions. For Cp_2M^+ , the following mean M-Cp bond disruption enthalpies (kcal mol⁻¹) are derived: $\Delta H_{hom}^\circ(M^+-Cp) = 95 \pm 3$ (V), 74 ± 4 (Mn), 91 ± 3 (Fe), 83 ± 3 (Ni); $\Delta H_{het}^\circ(M^{+3}-Cp) = 563 \pm 4$ (V), 604 ± 5 (Mn), 593 ± 4 (Fe), 659 ± 4 (Ni). Differential solvation free energies ($\Delta\Delta G_{solv}^\circ$) for several metallocene/metallocenium redox couples are derived. With the exception of $Cp_2V^{+/0}$, most of the first transition row metallocene/metallocenium redox couples are estimated to have $\Delta\Delta G_{solv}^\circ$ values of 38 ± 5 kcal mol⁻¹, which is consistent with the Born approximation for predicting ion solvation energies. These assessments of bonding and solvation energetics based on gas-phase adiabatic ionization energies lead to a complete thermochemical interpretation of observed solution electrode potentials for the metallocene redox couples studied.

Introduction

The thermochemistry of organometallic compounds has received increasing attention in recent years as investigators attempt to define the thermodynamic contributions to reactivity and catalysis.¹⁻³ Most of the thermochemical studies have focused on the use of combustion or reaction calorimetry to determine bond energetics for neutral complexes in the condensed phase and solution.² Gas-phase bond energy studies have often involved coordinatively unsaturated ionic metal species such as $M-R^+$ ($R = H, CH_3, CH_2, \text{etc.}$),⁴ but the stepwise bond energetics for complex organometallic ions such as $M(CO)_n^+$ have been determined with increasing accuracy by mass spectrometric methods.⁵ Other approaches involve the study of oxidation or reduction energetics in the gas phase⁶ or solution⁷ to provide key data for incorporation into thermochemical cycles leading to bond energies. In this article, we present results for the thermal ionization energetics of a number of prototypical metallocenes in the gas phase,⁸ and from this data mean bond disruption enthalpies and solvation free energies are derived for some of the metallocenium ions and $Cp_2M^{+/0}$ redox couples, respectively ($Cp = \eta^5$ -cyclopentadienyl). These results allow the full characterization of the thermochemical origins^{9,10} of the trends and absolute values of the observed

electrode potentials for these compounds.

The majority of data concerning metallocene oxidation-reduction thermochemistry are in the form of electrode potentials¹¹ and vertical ionization energies measured by photoelectron spectroscopy (PES).¹² These types of data are not always useful in deriving the thermodynamic properties of the ions near room temperature. Many of the common metallocenes have irreversible electrochemical oxidations and/or reductions, making determination of true $E_{1/2}$ values difficult.¹¹ A vertical ionization energy determined by PES will only be an accurate measurement of the adiabatic gas-phase ionization energy if the differences in equilibrium geometries of the ion and neutral complexes are small. Any structural changes that accompany ionization can result in a vertical ionization potential that differs significantly from the adiabatic ionization potential referenced at 0 K.¹³ In addition, even if the adiabatic ionization potential can be determined by PES, the enthalpy and free energy of ionization at other temperatures must be estimated by a statistical mechanical analysis based on spectroscopic data, which is often not available or incomplete.

The study of gas-phase electron-transfer equilibria (ETE) is a well-established approach for determining adiabatic ionization energetics for organic and inorganic species near room temperature.^{14,15} An earlier ETE study of the gas-phase ionization thermochemistry of ferrocene using pulsed high-pressure mass spectrometry (PHPMS) has been reported by Mautner.¹⁶ In the present study, Fourier transform ion cyclotron resonance mass

(1) (a) Martinho Simões, J. A. *Energetics of Organometallic Species*; NATO Advanced Study Institute Series C367; Kluwer: Dordrecht, 1992. (b) Marks, T. *Bond Energetics in Organometallic Compounds*; ACS Symposium Series 428; American Chemical Society: Washington, DC, 1990.

(2) Skinner, H. A.; Conner, J. A. *Pure Appl. Chem.* **1985**, *57*, 79.

(3) Beauchamp, J. L.; Martinho Simões, J. A. *Chem. Rev.* **1990**, *90*, 629.

(4) Armentrout, P. B. In *Bond Energetics in Organometallic Compounds*; Marks, T., Ed.; ACS Symposium Series 428; American Chemical Society: Washington, DC, 1990.

(5) (a) Schultz, R. H.; Crellin, K. C.; Armentrout, P. B. *J. Am. Chem. Soc.* **1991**, *113*, 8590 and references therein. (b) Sunderlin, L. S.; Wang, D.; Squires, R. R. *J. Am. Chem. Soc.* **1992**, *114*, 2788.

(6) Richardson, D. E. In *Energetics of Organometallic Species*; Martinho Simões, J. A., Ed.; NATO Advanced Study Institute Series C367; Kluwer: Dordrecht, 1992.

(7) (a) Bordwell, F. G.; Cheng, J. P.; Ji, G. Z.; Zhang, X. *J. Am. Chem. Soc.* **1991**, *113*, 9790 and references therein. (b) Parker, V. D.; Handoo, K. L.; Roness, F.; Tilset, M. *J. Am. Chem. Soc.* **1991**, *113*, 7493.

(8) Richardson, D. E.; Christ, C. S.; Sharpe, P.; Ryan, M. F.; Eyler, J. R. In *Bond Energetics in Organometallic Compounds*; Marks, T., Ed.; ACS Symposium Series 428; American Chemical Society: Washington, DC, 1990.

(9) Richardson, D. E. *Inorg. Chem.* **1990**, *29*, 3213.

(10) Buckingham, D. A.; Sargeson, A. M. In *Chelating Agents and Metal Chelates*; Dwyer, F. P., Mellor, D. P., Eds.; Academic: New York, 1964; p 237.

(11) Kotz, J. C. In *Topics in Organic Electrochemistry*; Fry, A. J., Britton, W. E., Eds.; Plenum Press: New York, 1986.

(12) Green, J. C. *Struct. Bonding (Berlin)* **1986**, *43*, 37.

(13) Lias, S. G.; Bartmess, J. E.; Liebman, J. F., Holmes, J. L., Levin, R. D., Mallard, W. G., Eds. *Gas-Phase Ion and Neutral Thermochemistry*; American Institute of Physics: New York, 1988.

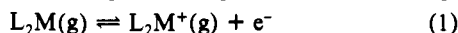
(14) (a) Lias, S. G.; Jackson, J. A.; Argenian, H.; Liebman, J. F. *J. Org. Chem.* **1985**, *50*, 333. (b) Meot-Ner (Mautner), M.; Nelsen, S. F.; Willi, M. R.; Frigo, T. B. *J. Am. Chem. Soc.* **1984**, *106*, 7384. (c) Nelsen, S. F.; Rumack, D. T.; Meot-Ner (Mautner), M. *J. Am. Chem. Soc.* **1988**, *110*, 7945.

(d) Lias, S. G.; Ausloos, P. *J. Am. Chem. Soc.* **1978**, *100*, 6027.

(15) Kebarle, P.; Chowdhury, S. *Chem. Rev.* **1987**, *87*, 513.

(16) Meot-Ner (Mautner), M. *J. Am. Chem. Soc.* **1989**, *111*, 2830.

spectrometry (FTICR-MS)¹⁷ is used to follow gas-phase electron-transfer reactions of ferrocene, other first transition row metallocenes, ruthenocene, and osmocene with a variety of reference compounds. From the measured equilibrium constants, K_{eq} , for the electron-transfer reactions, the free energies of reaction (ΔG_{et}°) are determined, and the free energies of ionization (ΔG_i°) for the metallocenes are estimated for the processes shown generally in eq 1, where L represents Cp or a substituted Cp.



Following established methods,^{8,18,19} we incorporated the ionization energy data into thermochemical cycles to provide estimates for mean bond disruption enthalpies for the metallocenium ions.

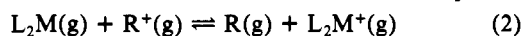
Ring substituent effects in the oxidation energies of cyclopentadienyl and arene complexes have previously been determined by using electrochemistry¹¹ and PES.¹² In the present study, the ETE method was applied to a number of alkylferrocenes to investigate the effect of alkyl substituents on gas-phase redox thermochemistry. The resulting ΔG_i° values are correlated with alkyl substituent parameters.²⁰ These data are potentially useful in the interpretation and prediction of substituent effects on the physical properties of metallocenes, such as ionization energies and optical transition energies. The latter property is important in the selection of chromophores for potentially useful nonlinear optical devices.²¹

Values for the entropy of ionization (ΔS_i°) and the enthalpy of ionization (ΔH_i°) for metallocenes are also estimated in this work from the temperature dependence of the equilibrium constants for selected electron-transfer equilibria. Entropies of ionization for some of the metallocenes (including ferrocene) are found to be larger than initially expected. Statistical mechanical estimates based on spectroscopic data for the $Cp_2Fe^{+/0}$ couple are used to estimate the intramolecular entropy contributions to the overall ionization entropy $\Delta S_i^\circ(Cp_2Fe)$. New vibrational data have been obtained for the ferrocenium ion to allow estimation of the intramolecular contributions to ΔS_i° for the prototypical $Cp_2Fe^{+/0}$ couple.

In contrast to the steadily improving situation for bond disruption enthalpies of organometallic compounds and ions, little is known about solvation energetics for organometallic redox couples.⁶ Such couples (particularly $Cp_2Fe^{+/0}$ and ferrocene derivatives) have been widely applied in experimental²² and theoretical²³ studies of electron-transfer phenomena. Thermochemical cycles are used here to derive differential free energies of solvation for several metallocene redox couples. The experimentally derived values are compared to predictions of simple ion solvation theory, and the comparison confirms some common views concerning the nature of metallocene/metallocenium-solvent interactions.

Results

Electron-Transfer Equilibria. The techniques used in ETE studies have been described extensively elsewhere.^{6,14,15} Figure 1 shows an example of typical ETE data obtained in this study. The general electron-transfer equilibria of eq 2 were studied, where L_2M is a metallocene and R denotes a reference compound.



(17) For reviews of the ion cyclotron resonance technique, see: (a) Marshall, A. G. *Acc. Chem. Res.* **1985**, *18*, 316. (b) Gross, M. L.; Rempel, D. L. *Science* **1984**, *226*, 261. (c) Eyler, J. R.; Baykut, G. *Trends Anal. Chem.* **1986**, *5*, 44.

(18) Beauchamp, J. L.; Stevens, A. E. *J. Am. Chem. Soc.* **1981**, *103*, 190.

(19) Sharpe, P.; Richardson, D. E. *J. Am. Chem. Soc.* **1991**, *113*, 8339.

(20) (a) Levitt, L. S.; Widing, H. F. *Prog. Phys. Org. Chem.* **1976**, *12*, 119. (b) Levitt, L. S.; Levitt, B. W. *J. Inorg. Nucl. Chem.* **1976**, *38*, 1907. (c) Parkanyi, C.; Levitt, L. S.; Levitt, B. W. *Chem. Ind.* **1977**, 356.

(21) Calabrese, J. C.; Cheng, L. T.; Green, J. C.; Marder, S. R.; Tam, W. *J. Am. Chem. Soc.* **1991**, *113*, 7227 and references therein.

(22) For example, see (a) Sohn, Y. S.; Hendrickson, D. C.; Gray, H. B. *J. Am. Chem. Soc.* **1971**, *93*, 3603. (b) McManis, G. E.; Nielson, R. M.; Gochev, A.; Weaver, M. J. *J. Am. Chem. Soc.* **1989**, *111*, 5533. (c) Nielson, R. M.; Golovin, J. D.; McManis, G. E.; Weaver, M. J. *J. Am. Chem. Soc.* **1988**, *110*, 1745. (d) Nielson, R. M.; Golovin, J. D.; McManis, G. E.; Weaver, M. J. *J. Chem. Phys.* **1988**, *92*, 3442.

(23) Newton, M. D.; Ohta, K.; Zhong, E. *J. Phys. Chem.* **1991**, *95*, 2317.

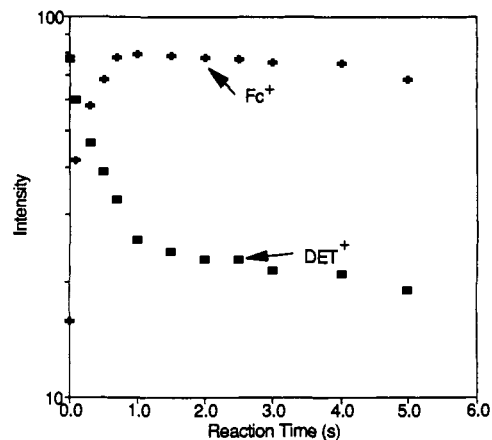


Figure 1. Log plot for the electron-transfer reaction $Cp_2Fe + DET^+ = DET + Cp_2Fe^+$ (arbitrary intensity units). DET = *N,N*-diethyltoluidine and Fc = ferrocene.

Equilibrium constants and free energies (ΔG_{et}°) can be established if the difference in the free energies of ionization for the two compounds, $\Delta\Delta G_i^\circ$, is sufficiently small ($\leq 3-4$ kcal mol⁻¹).¹³ Equilibria involving parent ions can actually be detected for ΔG_{et}° values approaching 5 kcal mol⁻¹, but the partial pressure ratio must then exceed 100, which leads to unacceptable experimental errors (the pressure of the minor component would be only slightly above background pressure). Since the free energy of ionization of reference compound R is known, the ΔG_i° value at temperature T of the other compound can be determined via eq 3.

$$\Delta G_{et,T}^\circ = \Delta G_{i,T}^\circ(L_2M) - \Delta G_{i,T}^\circ(R) \quad (3)$$

mination of ΔG_{et}° values over a temperature range allows estimation of ΔH_{et}° , ΔS_{et}° , and, if corresponding values are known for the reference compound, $\Delta H_i^\circ(L_2M)$ and $\Delta S_i^\circ(L_2M)$ values applicable in that temperature range can be derived.

Reference compounds suitable for ETE studies in the 6–7-eV range of ionization energies have been investigated by both PHPMS and ion cyclotron resonance mass spectrometry.¹⁴ From the data in the literature,¹⁴ we established a series of reference compounds with ionization thermodynamics based on the following assumptions: (i) $\Delta H_i^\circ(\text{dimethylaniline,DMA}) = 7.12 \pm 0.02$ eV.¹³ (ii) ΔS_i° for azulene results only from ΔS_{elec} (for the singlet to doublet process, $\Delta S_i^\circ = R \ln 2 = 1.38$ cal mol⁻¹ K⁻¹). (iii) From the reported ΔS_{et}° value for the ETE involving DMA and azulene, $\Delta S_i^\circ(\text{DMA}) = 2.3$ cal mol⁻¹ K⁻¹.^{14c} (iv) All *N,N*-alkylanilines have the same ΔS_i° value as DMA. (v) Changes in heat capacity accompanying ionizations of the reference compounds are negligible^{14d} and tend to cancel in the ΔC_p term. Therefore, derived ΔH_i° values are assumed independent of temperature in the range 350–550 K.

Assumption i has been used as an anchor for previous studies involving the present reference compounds.^{14,16} Assumption ii is reasonable in view of the small vibrational and rotational entropy changes expected for the ionization of azulene. The small, positive values of ΔS_i° used for the *N,N*-alkylanilines in assumptions iii and iv are reasonable and presumably are composed of the electronic entropy change plus small contributions from rotational and vibrational degrees of freedom. The relatively minor ΔC_p effects on ΔH_i° (assumption v) have been discussed elsewhere.^{14d}

Figure 2 is an equilibrium ladder displaying all the electron-transfer reactions studied at 350 K in this work.^{8,24} Each equilibrium constant determination was repeated at least three times, and the reactions were studied from both endoergic and exoergic directions to demonstrate that the equilibrium constants obtained are not dependent upon the direction of approach to equilibrium. Arrows denote ETE reactions reported in this work,

(24) The derived values of ΔG_i° for the metallocenes differ somewhat from those given for some of the compounds in preliminary reports of this work.⁸ The differences arise from the use of new values for the reference compounds as described in the text and more extensive experimental ETE data.

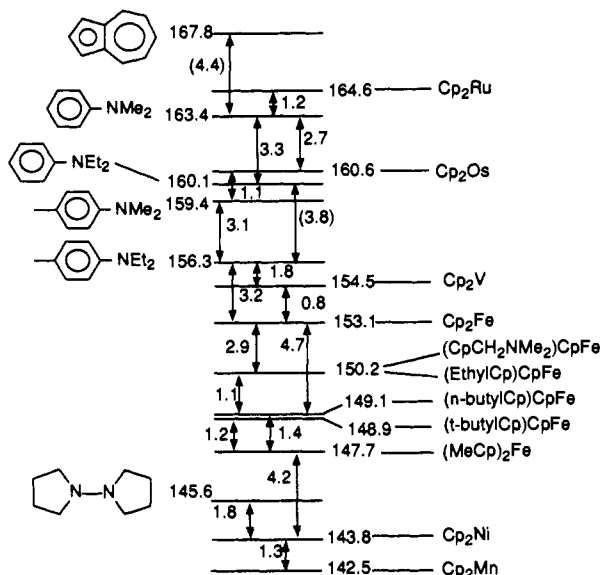


Figure 2. Free energy of ionization ladder for a series of metallocenes. Values reported in kcal mol⁻¹. The $\Delta G_{\text{et}}^{\circ}$ values are adjacent to arrows connecting neutral reactants. All $\Delta G_{\text{et}}^{\circ}$ values are referenced at 350 K and are anchored to $\Delta G_{\text{et}}^{\circ}(\text{DMA})$. See text for assumptions used for reference ionization free energies.

Table I. Ionization Energetics Data for Some Metallocenes

Cp ₂ M	$\Delta G_{\text{et}}^{\circ a,b}$	$\Delta H_{\text{et}}^{\circ a}$	$\Delta S_{\text{et}}^{\circ c}$	vIP (PES) ^d
Cp ₂ V	154.5	~154	~0 ± 0.3 ^d	155.7 ^e
Cp ₂ Fe	153.1	157.2	11.6 ^f	158.2 ^g
Cp ₂ Mn	142.5			159.3 ^g
Cp ₂ Ni	143.8			149.9 ^g
Cp ₂ Ru	164.6	~166	~5 ^h	171.8 ^g
Cp ₂ Os	160.6	~162	~5 ^h	164.9 ⁱ

^a Units are kcal mol⁻¹. ^b At 350 K. Estimated error limits ±1.5 kcal mol⁻¹. ^c Units are cal mol⁻¹ K⁻¹. ^d $\Delta S_{\text{et}}^{\circ}$ depends on uncertain ion ground state (ref 25b). ^e Reference 37. ^f Determined from a van't Hoff plot for the Cp₂Fe/DET couple assuming $\Delta S_{\text{et}}^{\circ}(\text{DET})$ is 2.3 cal mol⁻¹ K⁻¹. ^g Reference 25c. ^h Value assumed to be equal to statistical mechanics value for $\Delta S_{\text{et}}^{\circ}(\text{Cp}_2\text{Fe})$. ⁱ Reference 36.

with derived $\Delta G_{\text{et},350}^{\circ}$ values adjacent to the arrows. Some electron-transfer reactions involving only reference compounds were conducted as checks on the reported literature values. In all cases, the experiments were in good agreement with the literature values, and the free energy changes for these comparisons are shown on the ladder. Values in parentheses denote reactions involving reference compounds that were not checked and are used here as previously reported. Table I lists the $\Delta G_{\text{et}}^{\circ}$ values for the Cp₂M compounds. An error limit of ±1.5 kcal mol⁻¹ is assigned to the $\Delta G_{\text{et}}^{\circ}$ values based upon experimental errors in the measured partial pressures of the neutral gases and errors in the $\Delta G_{\text{et}}^{\circ}$ of the organic reference compounds.¹⁴

The free energies of ionization of Cp₂Ni and Cp₂Mn are significantly lower than the $\Delta G_{\text{et}}^{\circ}$ values of the other metallocenes, and the aniline derivatives are not useful reference compounds. Therefore, nickelocene and manganocene have been anchored to the hydrazine derivative 1,1'-bipyrrrolidine, which has previously been anchored to *N,N*-dimethylaniline.^{14d} Nelsen et al. suggested a value for $\Delta H_{\text{et}}^{\circ}(1,1'\text{-bipyrrrolidine})$ of 146.9 kcal mol⁻¹ from PHPMS ETE studies.^{14c} We have chosen a value of 145.8 kcal mol⁻¹ for $\Delta G_{\text{et},350}^{\circ}(1,1'\text{-bipyrrrolidine})$ by using the assumptions above. In addition to this reference compound, the ferrocene alkyl derivatives also extend the ladder from the aniline derivatives to Cp₂Ni and Cp₂Mn (Figure 2), and the internal agreement is very good (±0.3 kcal mol⁻¹).

The temperature dependencies of electron-transfer equilibrium constants for three reactions are shown on van't Hoff plots in Figure 3. Derived thermodynamic parameters are given in Table I. Included in Table I are estimates for enthalpies and entropies of ionization of the metallocenes based on the present data.

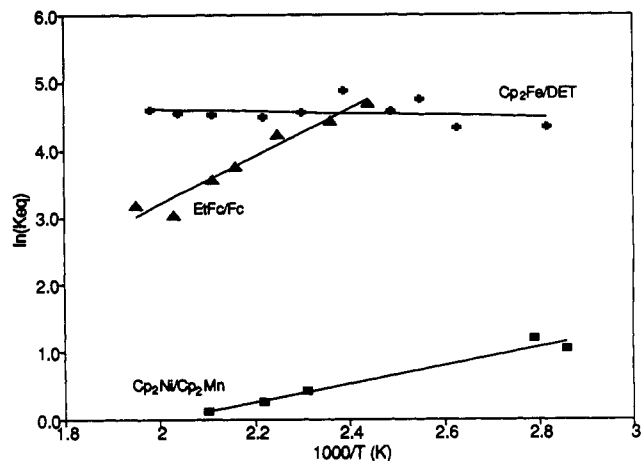


Figure 3. van't Hoff plots for selected metallocene electron-transfer reaction couples. Values for $\Delta H_{\text{et}}^{\circ}$ and $\Delta S_{\text{et}}^{\circ}$ are given in the text. DET = *N,N*-diethyltoluidine, Fc = ferrocene, EtFc = ethylferrocene, Cp₂Mn = manganocene, and Cp₂Ni = nickelocene.

Table II. Vibrational Frequencies for Various Ferrocenium Salts

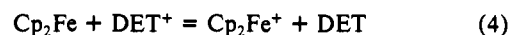
compd	frequency (ν_{22}) Cp-Fe-Cp bend, cm ⁻¹	$S^{\circ}(\nu_{22})^a$ cal mol ⁻¹ K ⁻¹
(Cp ₂ Fe ⁺)(Cl ⁻)	135	5.7
(Cp ₂ Fe ⁺)(BF ₄ ⁻)	140	5.6
(Cp ₂ Fe ⁺)(PF ₆ ⁻)	130	5.8
Cp ₂ Fe	179	4.7

^a Contribution of ν_{22} doubly degenerate mode to vibrational entropy at 298 K.

Far-Infrared Spectroscopy. Various ferrocenium ion salts and ferrocene were examined in polyethylene pellets in the spectral region 50–750 cm⁻¹. Band frequencies are summarized in Table II. A band found in all of the [Cp₂Fe]X (X = Cl, PF₆, or BF₄) spectra at 135 cm⁻¹ has been tentatively assigned as the previously unreported Cp-Fe-Cp bending mode, which was confirmed to occur at 179 cm⁻¹ in ferrocene.

Discussion

Ferrocene. The electron-transfer equilibrium reaction of ferrocene with *N,N*-diethyltoluidine, DET, (eq 4) has been investigated previously by using PHPMS,¹⁶ and from the published data we have estimated that $\Delta G_{\text{et},350}^{\circ} = -0.9$ kcal mol⁻¹. Mautner's data¹⁶ cover a temperature range of ~450–650 K, and the thermodynamic parameters have been extrapolated to 350 K, the temperature at which the most extensive FTICR studies were performed. The estimated value from the present FTICR studies



for $\Delta G_{\text{et},350}^{\circ}$ (eq 4) is -3.2 kcal mol⁻¹, and the derived value for $\Delta G_{\text{et},350}^{\circ}(\text{Cp}_2\text{Fe}) = 153.1 \pm 1.5$ kcal mol⁻¹ (Figure 2). The difference in the PHPMS and FTICR values for $\Delta G_{\text{et}}^{\circ}$ (eq 4) is much larger than normally expected in such comparisons and led us to study this equilibrium in more detail.

Since the temperature dependence of the equilibrium constant for eq 4 was measured by using PHPMS¹⁶ (fit to $\Delta H_{\text{et}}^{\circ} = -0.1$ kcal mol⁻¹ and $\Delta S_{\text{et}}^{\circ} = 2.2$ cal mol⁻¹ K⁻¹ for in the range 450 < T < 650 K), we also studied the temperature dependence of eq 4 to investigate the origin of the difference in $\Delta G_{\text{et}}^{\circ}$ values and to provide FTICR data in a temperature range that overlaps with the PHPMS study. The range of temperatures employed in the present work was 350–520 K. The van't Hoff plot (Figure 3) for eq 4 demonstrates a minor temperature dependence, and derived thermodynamic parameters are $\Delta H_{\text{et}}^{\circ} = 0.05 \pm 0.47$ kcal mol⁻¹ and $\Delta S_{\text{et}}^{\circ} = 9.3 \pm 1.1$ cal mol⁻¹ deg⁻¹. The derived values of $\Delta H_{\text{et}}^{\circ}$ (eq 4) for both the PHPMS and FTICR-MS studies are within experimental error of each other, but the $\Delta S_{\text{et}}^{\circ}$ (eq 4) value determined by FTICR is significantly more positive than the PHPMS value. The observed differences in $\Delta G_{\text{et}}^{\circ}$ (eq 4) values clearly originate in the entropy term. The larger equilibrium

Table III. Calculated Entropies^a and Integrated Heat Capacities^b for Ferrocene and Ferrocenium Ion at 298, 450, and 600 K

	Cp ₂ Fe (298 K)	Cp ₂ Fe ⁺ (298 K)	Cp ₂ Fe (450 K)	Cp ₂ Fe ⁺ (450 K)	Cp ₂ Fe (600 K)	Cp ₂ Fe ⁺ (600 K)
S ^o _{trans}	41.6	41.6	43.6	43.6	45.0	45.0
S ^o _{rot^c}	24.3	24.4	25.5	25.6	26.4	26.6
S ^o _{int rot}	5.24	5.24	5.75	5.75	6.12	6.12
S ^o _{vib^d}	14.88	17.19	30.17	32.97	45.84	48.89
S ^o _{elec^{e,f}}	¹ A _{1g} q = 1 S ^o = 0	² E _{2g} q = 2.07 S ^o = 1.67	¹ A _{1g} q = 1 S ^o = 0	² E _{2g} q = 2.22 S ^o = 2.02	¹ A _{1g} q = 1 S ^o = 0	² E _{2g} q = 2.38 S ^o = 2.25
S ^o _{total}	85.5	90.1	105.0	109.9	122.8	128.9
ΔH ^o _T - ΔH ^o _{0K}	5.3	5.7	12.3	13.0	21.7	22.6

^a Units are cal mol⁻¹ K⁻¹. ^b Units are kcal mol⁻¹. ^c Entropy of rotations calculated assuming Cp-Fe is as a linear rigid rotor. ^d Vibrational entropy was calculated for all vibrational modes. See text. ^e S^o_{elec,T} = -Rln(q) + E_{therm,T}. ^f The ²E_{2g} state is split into two Kramer's doublets. Ignoring low-symmetry contributions, the estimated splitting due to spin-orbit coupling is ~700 cm⁻¹. See Prins, R. *Mol. Phys.* 1970, 19, 603.

constant for eq 4 in the FTICR study is consistent with our inability to observe ETE of the Cp₂Fe⁺⁰ couple with dimethyltoluidene (DMT), where an estimated ΔG_{et,350}^o value of >5 kcal mol⁻¹ would be expected. The same ferrocene/DMT equilibrium was observed in the PHPMS study with an estimated ΔG_{et,429}^o = -3.6 kcal mol⁻¹.¹⁶

Based on the assumptions used to construct our ionization energy ladders, we derive a value for ΔH_i^o(Cp₂Fe) = 157.2 ± 1.5 kcal mol⁻¹ (6.82 eV), which is 0.01 eV higher than the value suggested by Mautner only because of the difference in his selected reference value for ΔH_i^o(DET) and ours (152.7 kcal mol⁻¹). Considering the usual errors associated with ETE experiments in both FTICR and PHPMS, the adiabatic ionization energy (aip) values for ferrocene estimated by both methods are in agreement and can be given as 6.82 ± 0.08 eV. For comparison, the vertical IP of ferrocene has been measured at 6.88 ± 0.02 eV by various groups.^{12,25} Unfortunately, vibrational fine structure has not been consistently resolved in the PES spectrum of Cp₂Fe(g),^{12,25} and therefore the aip value is not readily extracted from the photoelectron data (unlike the case for osmocene discussed below).

In contrast to the situation for the enthalpy of ionization of ferrocene, the correct value for the entropy change accompanying eq 4 is not clear given the significant differences in the FTICR-MS and PHPMS results. Several observations support the higher entropy value derived in the present work, but it has not been possible to completely establish which value is more correct. We have investigated the temperature dependence of other ETE equilibria involving molecules and ions with well-established thermodynamic constants and generally derive ΔS_{et}^o values within ±2 cal mol⁻¹ K⁻¹ of the expected value (e.g., for CO⁺⁰/Kr⁺⁰ and benzoquinone^{0/-}/*p*-cyanonitrobenzene^{0/-}).⁶ The derived ΔS_{et}^o value for the (EtCp)CpFe/Cp₂Fe ETE is within experimental error of zero, which would be expected for ETE involving these structurally similar reactants (see below). In general, equilibrium constants determined at 350 K for ETE between the organic reference compounds (Figure 2) are well within experimental error (±1.5 kcal mol⁻¹) of values determined previously by PHPMS or ICR methods. The ladder in Figure 2 connects DET and 1,1'-bipyrrrolidine, which have been previously linked in PHPMS study by Mautner and co-workers, via ferrocene and its derivatives. The derived free energy ladder in this region is self consistent within 0.3 kcal mol⁻¹. These various observations suggest that FTICR equilibrium constants involving the metallocenes and the reference compounds do not have large random errors.

A possible explanation for the difference between equilibrium constants for eq 4 as determined by FTICR and PHPMS would involve inaccurately measured ion intensity ratios due to differences in ion detection sensitivity. In the case of the FTICR experiment, we have analyzed total ion counts (I(Fc⁺) + I(DET⁺)) as a function of time and find only minor (~10%) changes during the

period in which the I(Fc⁺)/I(DET⁺) ratio is changing rapidly in approach to equilibrium. It is unlikely that systematic detection errors contribute significantly to errors in either type of experiment.

The most likely source of error in ETE equilibrium constants is in the measurement of neutral pressures. Since different methods are used to establish reactant pressures in PHPMS and FTICR-MS, it is conceivable that systematic errors in these pressures are introduced in one or both of the experiments. The difference between ΔS_{et}^o (eq 4) values for the two experiments is equivalent to a pressure error factor of ~25 (derived enthalpy changes are not affected by pressure measurements errors; thus, it is not surprising that the two methods are in agreement on the ΔH_{et}^o (eq 4) values).²⁶

One method used to validate measured or calculated pressures is to determine rate constants for ion/molecule reactions that are expected to be near collision controlled. Mautner reports a k_f value for eq 4 at 461 K of 1.2 × 10⁻⁹ cm³ s⁻¹, while we have determined a k_f value (450 K) of 2.5 × 10⁻¹⁰ cm³ s⁻¹. The former rate constant is at or slightly above the Langevin collision limit, while the FTICR k_f is about 25% of the Langevin rate constant.²⁷ These rate comparisons, which differ by a factor of ~5, do not resolve the disagreement. For example, if one accepts the PHPMS equilibrium constants for eq 4, it would require that the P(Fc)/P(DET) ratio be underestimated by a factor a ~25 in the FTICR experiment; in turn, this underestimation would lead to an overestimation of k_f from FTICR data by up to a factor of ~25 depending on the absolute errors in the P(DET) and P(Fc) measurements. Thus, the k_f value from the two experiments would diverge if the P(Fc) in the FTICR experiment was underestimated.

From other studies involving rates of electron-transfer reactions of metallocenes, it seems unlikely that such large errors in established pressure ratios could occur in the FTICR experiment. The same methods used here have been applied in determination of electron-transfer rate constants for a number of metallocene self-exchange and cross reactions,^{28a} and the estimated reaction efficiencies for the most exothermic cross reactions were in the range 0.5–1.5, which suggests absolute pressure errors no larger than 50% if the reactions truly occur at the collision rate (efficiency = 1). The observation of an efficiency of ~0.2 for the forward reaction in eq 4 is not unexpected for a reaction with relatively low exoergicity involving ferrocene, which has a FTICR-determined self-exchange rate constant below the collisional limit.²⁸ In the same way, however, it does not seem likely that such large pressure errors would occur in the PHPMS experiment, the ferrocene apparently does not decompose in the temperature range

(26) In the FTICR method, pressures are read directly from an ion gauge that has been calibrated against a capacitance manometer for each reactant gas. In the PHPMS method, a mixture containing known amounts of reactants is introduced into a heated bulb and the relative pressures of the reactants in the source gas are calculated. In the FTICR experiment, the ion gauge is remote from the ion trap due to the magnetic field, so pressures at the ion trap must be deduced from calibration experiments under static and pumped conditions in the vacuum chamber (see Experimental Section).

(27) Su, T.; Bowers, M. T. In *Gas-Phase Ion Chemistry*; Bowers, M. T., Ed.; Academic: New York, 1979; Vol. 2.

(28) (a) Richardson, D. E.; Christ, C. S.; Sharp, P.; Eyer, J. E. *J. Am. Chem. Soc.* 1987, 109, 3894. (b) Phelps, D. K.; Gord, J. R.; Frieser, B. S.; Weaver, M. J. *J. Phys. Chem.* 1991, 95, 4338.

(25) (a) Evans, S.; Green, M. L. H.; Jewitt, B.; Orchard, A. F.; Pygall, C. F. *J. Chem. Soc., Faraday Trans. 2* 1972, 68, 1847. (b) Evans, S.; Green, M. L. H.; Jewitt, B.; King, G. H.; Orchard, A. F. *J. Chem. Soc., Faraday Trans. 2* 1974, 70, 356. (c) Cauletti, C.; Green, J. C.; Kelly, R.; Powell, P.; Van Tilborg, J.; Robbins, J.; Smart, J. *J. Electron Spectrosc. Relat. Phenom.* 1980, 19, 327. (d) Rabalais, J. W.; Werme, L. O.; Karlson, L.; Hussain, M.; Siegbahn, K. *J. Chem. Phys.* 1972, 57, 1185.

Table IV. Auxiliary Thermochemical Data Used in Thermochemical Cycles^a

process	V	Mn	Fe	Ni
$\Delta H_i^\circ[\text{Cp}_2\text{M}]^b$	49 ± 2	66 ± 2	58 ± 1	85 ± 1
$\Delta H_i^\circ[\text{M}]^c$	123 ± 2	67 ± 2	99 ± 2	103 ± 2
$\Delta H_i^\circ[\text{M}^+]^c$	278 ± 2	238 ± 2	281 ± 2	279 ± 2
$\Delta H_i^\circ[\text{M}^{2+}]^c$	616 ± 2	599 ± 2	654 ± 2	698 ± 2
$\Delta H_i^\circ[\text{M}^{3+}]^c$	1292 ± 2	1376 ± 2	1361 ± 2	1509 ± 2
$\Delta H_i^\circ[\text{Cp}]^b = 58 \pm 1$				
$\Delta H_i^\circ[\text{Cp}^-]^b = 19.6 \pm 4$				

^a Units are kcal mol⁻¹. ^b Reference 13. ^c Reference 44.

used.²⁹ Thus, kinetic results do not resolve the origin of the discrepancy.

Intramolecular Entropy and the Ferrocene/Ferrocenium Couple.

Given the experimentally uncertain entropy changes for the Cp₂Fe couple, we have performed a detailed statistical mechanical analysis to provide an estimate of the value of $\Delta S_i^\circ(\text{Cp}_2\text{Fe}^{0/+})$. Table III lists the calculated entropy values for translational, rotational, vibrational, and electronic entropies for ferrocene and the ferrocenium cation.³⁰ Published vibrational frequencies of ferrocene³¹ and ferrocenium ion^{32,33} were used in vibrational entropy analysis. Bodenheimer and Low³¹ report frequency assignments for all 57 vibrational modes of ferrocene.

As noted elsewhere,³⁴ low-frequency metal-ligand bending modes can contribute significantly to redox entropy changes for metal complexes if the frequency shifts significantly upon change in oxidation state. The doubly degenerate Cp-Fe-Cp bend for the ferrocenium ion has not been reported previously, but the corresponding mode for Cp₂Fe has a relatively low frequency, $\nu_{22} = 179 \text{ cm}^{-1}$.³¹ Our far-IR study (Table II) confirmed the latter frequency and located a new band of comparable intensity at $\sim 135 \text{ cm}^{-1}$ in ferrocenium salts. It was expected that the bending mode would move to lower frequency in the cation since the Cp-Cp distance increases³⁵ and the metal ligand force constants generally decrease from ferrocene to the ferrocenium ion. This single shift in the bending mode contributes $\sim 1.0 \text{ cal mol}^{-1} \text{ K}^{-1}$ to the estimated value of $\Delta S_i^\circ(\text{Cp}_2\text{Fe}^{0/+})$ in the temperature range 298–600 K.

Combining the calculated value of $\Delta S_i^\circ(\text{Cp}_2\text{Fe}^{0/+})$ at 450 K (5.1 cal mol⁻¹ K⁻¹) with the assumed value of $\Delta S_i^\circ(\text{DET}^{0/+})$ (2.3 cal mol⁻¹ K⁻¹), the estimated value for ΔS_{et}° (eq 4) is 2.8 cal mol⁻¹ K⁻¹, which is consistent with the value obtained in the previous PHPMS study (2.2 cal mol⁻¹ K⁻¹).¹⁶ Assuming statistical mechanics provides a good estimate for $\Delta S_i^\circ(\text{Cp}_2\text{Fe}^{0/+}(\text{g}))$, this analysis therefore supports the earlier PHPMS temperature dependence study of the reaction in eq 4. However, use of solid-state frequencies for the gas-phase ferrocenium ion may not be valid, so the estimated ΔS_i° value may be significantly different from the true value.

The temperature dependence of Cp₂Fe/(EtCp)CpFe (Figure 3) leads to $\Delta S_{et}^\circ = 0.96 \pm 3.6 \text{ cal mol}^{-1} \text{ K}^{-1}$. Since the substitution of an ethyl group for a hydrogen would be expected to lead to little change in the various contributions to ΔS_i° (Table IV), it is not surprising that this ETE has an entropy of ionization near 0.

Because of changes in the difference in the integrated heat capacities of Cp₂Fe and Cp₂Fe⁺ as a function of temperature, enthalpies of ionization will not be constant over the temperature

range of the various studies (Table III). However, the estimated variation in $\Delta H_i^\circ(\text{Cp}_2\text{Fe}^{0/+})$ is ca. 0.5 kcal mol⁻¹ in going from 298 to 600 K. Thus, the effect of the heat capacities in the comparisons of PHPMS and FTICR data is insignificant given the error limits of the data.

Ruthenocene and Osmocene. From previous physical and theoretical studies, the neutral ground-state electronic configuration for these complexes of the iron triad is ¹A_{1g}, assuming D_{5d} symmetry, and the electron configuration for the monocations is ²E_g.²⁵ The observed trend for the values of free energies of ionization for the iron triad metallocenes parallels that observed for the vertical ionizations (IP Cp₂Fe < Cp₂Os < Cp₂Ru).^{25,34} Table I lists values for the thermal free energies of ionization and vertical ionization energies for the iron series of metallocenes as well as Cp₂Ni, Cp₂Mn, and Cp₂V.

Lichtenberger and Copenhagen³⁶ were able to obtain vibrational fine structure in the first ionization spectrum of osmocene that could be fit with an average 41.2-meV (332-cm⁻¹) spacing between vibrational levels in the cation and an aIP value for Cp₂Os of 161.1 kcal mol⁻¹.³⁶ Assuming a similar ΔS_i° for osmocene as derived from statistical mechanics for ferrocene above, the estimated osmocene aIP from ETE studies is $\sim 162 \text{ kcal mol}^{-1}$; thus, the two techniques are in agreement within experimental error.

Vanadocene, Nickelocene, and Manganocene. The sharpness of the first ionization band in the photoelectron spectrum of Cp₂V indicates that the difference in equilibrium geometries between the neutral and the ion is small.^{25,37} A recent PES of vanadocene³⁷ assigns the vIP at 155.7 kcal mol⁻¹ with 0.1 kcal mol⁻¹ resolution. Since the vertical ionization of vanadocene is a sharp band (total width = 0.19 eV), the aIP is closely approximated by the vIP. From our ETE data, the ΔG_i° value is 154.5 kcal mol⁻¹, and assuming that the ΔS_i° value is predominantly electronic in origin (i.e., negligible rotational and vibrational contributions) and therefore only moderately negative, ΔH_i° is estimated as $\sim 154 \pm 2 \text{ kcal mol}^{-1}$. Thus estimated value is on the low energy side of the PES band but within the band envelope.

Manganocene is of particular interest because it is predominantly a high-spin compound^{38,39} with a ⁶A(e_{2g})²(a_{1g})¹(e_{1g})² ground-state configuration in the gas-phase²⁵ while other metallocenes are invariably low-spin.³⁵ The PES of ⁶A manganocene has a broad first ionization band associated with a large geometry change upon ionization. Evans and workers^{25a} reported the vIP of manganocene as 144.4 kcal mol⁻¹, which was later confirmed by Green.^{25c} Because of spin selection rules, the vIP for the high-spin form is assigned to the ⁶A → ⁵E transition in which the cation is in the high-spin configuration. However, the ground state of the cation is expected to be low spin ³E, and the change in ring-centroid to metal distance is estimated to be 0.25 Å for Cp₂Mn(⁶A)/Cp₂Mn(³E) using the isoelectronic chromocene structure to estimate the M-Cp distance of the ion.⁴⁰ The substantial difference between the ETE value for ΔG_i° (142.5 kcal mol⁻¹) and the vIP (159.3 kcal mol⁻¹) suggests the largest relaxation energy for any of the metallocenes studied, $\sim 17 \text{ kcal mol}^{-1}$. The lower energy ³E ground state for Cp₂Mn⁺ is actually observed in the PES as a small component due to the small equilibrium amount of low-spin ³E Cp₂Mn in the gas-phase sample.^{25c} This ²E → ³E transition has a vIP of $\sim 144.4 \text{ kcal mol}^{-1}$.^{25c} From the relatively small energy difference between the high-spin and low-spin neutrals (which are in equilibrium), the overall Cp₂Mn(⁶A)/Cp₂Mn(³E) energy difference can be estimated from PES data as 144 kcal mol⁻¹, which is in substantial agreement with the ETE value of 143 kcal mol⁻¹. It is clear that use of the PES vIP data for the high-spin form in thermochemical calculations would lead to large errors in derived values of bond

(29) Lewis, K. E.; Smith, G. P. *J. Am. Chem. Soc.* 1984, 106, 4650.

(30) Because a complete vibrational analysis for Cp₂Fe⁺ has not yet been performed, several vibrational frequencies for the cation were estimated from the known vibrations of ferrocene and ferrocenium as follows. From vibrational frequencies that were measured in both the neutral and the cation, the percent change in the vibrational force constant was calculated. The percent change in the force constant was then applied to estimate a vibrational frequency for the analogous mode in the cation which has not been reported. Because of the importance of the low-frequency skeletal mode, the frequency of the Cp₂Fe⁺ Cp-Fe-Cp stretch was measured rather than estimated (see text).

(31) Bodenheimer, J. S.; Low, W. *Spectrochim. Acta* 1973, 29A, 1733.

(32) Duggan, M. D.; Hindrickson, D. N. *Inorg. Chem.* 1975, 14, 955.

(33) Pavlik, I.; KLIKORKA, J. *Coll. Czech. Chem. Commun.* 1991, 30, 664.

(34) Richardson, D. E.; Sharpe, P. *Inorg. Chem.* 1991, 30, 1412.

(35) Haaland, A. *Acc. Chem. Res.* 1979, 12, 415.

(36) Lichtenberger, D. L.; Copenhagen, A. S. *J. Chem. Phys.* 1989, 91, 663.

(37) Lichtenberger, D. L.; Rempe, M. E. Private Communication.

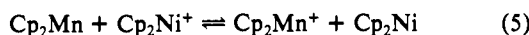
(38) Ammeter, J. H.; Bucher, R.; Oswald, N. *J. Am. Chem. Soc.* 1974, 96, 7833.

(39) Switzer, M. E.; Wang, R.; Rettig, M. F.; Maki, A. H. *J. Am. Chem. Soc.* 1974, 96, 7669.

(40) Richardson, D. E. *J. Chem. Phys.* 1986, 90, 3697.

energies and energies of formation for the Cp_2Mn^+ ion.

Since the spin-state change accompanying the ionization of Cp_2Mn is expected to lead to a relatively large decrease in metal-ligand vibrational frequencies and rotational moments, it was anticipated that the $\Delta S_1^\circ(\text{Cp}_2\text{Mn})$ value would be strongly negative. To confirm this large intramolecular entropy change, the temperature dependence of the $\text{Cp}_2\text{Ni}/\text{Cp}_2\text{Mn}$ electron-transfer reaction couple was investigated, and the van't Hoff plot for the reaction in eq 5 is shown in Figure 3. The enthalpy and



entropy changes for the reaction are $-3.2 \pm 1.5 \text{ kcal mol}^{-1}$ and $-5.7 \pm 3 \text{ cal mol}^{-1} \text{ K}^{-1}$, respectively. The negative $\Delta S_{\text{et}}^\circ$ is consistent with an overall negative $\Delta S_1^\circ(\text{Cp}_2\text{Mn})$ since the change in electronic configuration for the ionization of Cp_2Ni ($^3\text{A} \rightarrow ^2\text{E}$) would presumably lead to a lower magnitude for $\Delta S_1^\circ(\text{Cp}_2\text{Ni})$ compared to that of manganocene. Insufficient vibrational spectroscopy data are available to provide an independent statistical estimate of the vibrational contribution to $\Delta S_1^\circ(\text{Cp}_2\text{Mn})$ as done above for ferrocene; however, the frequencies are expected to increase markedly upon oxidation leading to a negative contribution to $\Delta S_1^\circ(\text{Cp}_2\text{Mn})$. Although manganocene oxidation occurs with a spin conversion ($^6\text{A} \rightarrow ^3\text{E}$) that suggests a total 6-fold electronic degeneracy in both neutral and ion, the electronic entropy of Cp_2Mn is greater than that of Cp_2Mn^+ because of spin-orbit splitting of the ^3E state of the ion. The rotational entropy change for the electron-transfer reaction is estimated to contribute -0.6 eu to $\Delta S_1^\circ(\text{Cp}_2\text{Mn})$ based on the estimated change in Mn-Cp distance accompanying ionization ($\sim 0.25 \text{ \AA}$). Thus, the estimated vibrational, electronic, and rotational contributions to $\Delta S_1^\circ(\text{Cp}_2\text{Mn})$ are all negative and are consistent with the negative entropy change derived for eq 5.

Substituent Effects in Ferrocene Derivative Oxidations. Despite the extensive studies of metallocene PES, surprisingly little is known about substituent effects in gas-phase metallocene oxidation thermochemistry.¹² Therefore, various ferrocene derivatives were studied by the ETE method in order to assess the effect alkyl substituents attached to the cyclopentadienyl ring have on the free energies of ionization. It is well-known from PES data that dimethylation or permethylation of metallocenes lowers the ionization energies.¹² Attachment of alkyl groups on the metallocene rings stabilizes the molecular cation relative to the neutral compound, thus lowering the free energy of ionization of the derivative with respect to the parent metallocene. Equilibrium results for alkylferrocene derivatives studied in the present work are shown in Figure 2.

Molecular ionization potentials of organic and organometallic compounds have been correlated previously with Taft substituent parameters.²⁰ The aliphatic σ_1 parameters were derived originally for substituted acetic acids,⁴¹ but they have been used successfully to correlate IP data.^{20a} For example, a plot of IP for $(\eta^6\text{-C}_6\text{H}_5\text{R})\text{chromiumtricarboxyl}$ derivatives versus $\sigma_1(\text{R})$, where R is an attached alkyl substituent, shows a strong correlation line.²⁰ The equation used by Levitt and co-workers²⁰ is given in eq 6,

$$\text{IP}(\text{M-R}) = a_1\sigma_1(\text{R}) + \text{IP}(\text{M}) \quad (6)$$

where $\text{IP}(\text{M-R})$ and $\text{IP}(\text{M})$ are the ionization potentials for the derivative and the parent compound respectively, σ_1 is the Taft parameter for R, and a_1 is the slope of the line. The Taft parameters for H is 0, and thus the substituent effects are referenced to hydrogen.^{20a} The slope a_1 indicates the sensitivity of the ionization process to the change in substituents.

A plot employing eq 6 for the ferrocene derivatives is shown in Figure 4. The slope of the line is $57 \pm 6 \text{ kcal mol}^{-1}$, which can be compared to that for the $(\eta^6\text{-C}_6\text{H}_5\text{R})\text{Cr}(\text{CO})_3$ compounds, $a_1 = 34.6 \text{ kcal mol}^{-1}$, and alkylbenzenes, $a_1 = 109.3 \text{ kcal mol}^{-1}$.²⁰ Alkylferrocene ionization energies are nearly twice as sensitive to changes in alkyl substituents as the chromium arene complexes

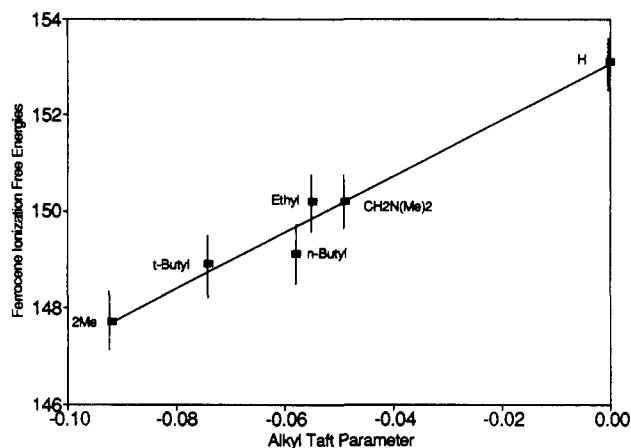


Figure 4. Plot of ΔG_1° (kcal mol $^{-1}$) versus alkyl Taft parameters (σ_1) for several ferrocene derivatives. Asterisk indicates new Taft parameter for $\text{CH}_2\text{N}(\text{CH}_3)_2$.

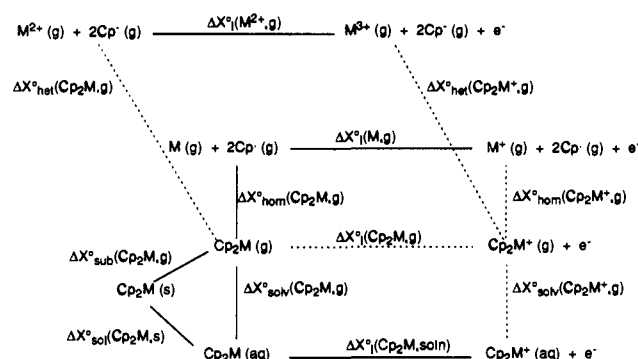


Figure 5. Thermochemical cycles used to determine bond disruption enthalpies and differential solvation free energies for metallocenes (solvent shown here is water). The upper portion of the cycle yields estimates for the average homolytic and heterolytic M-Cp bond disruption enthalpies. Comparison of $\Delta G_1^\circ(\text{g})$ and $\Delta G_1^\circ(\text{soln})$ in the lower portion of the cycle yields $\Delta\Delta G_{\text{soliv}}^\circ$ values for $\text{Cp}_2\text{M}^{+/0}$ couples. Dotted lines denote data resulting from this work.

but are less affected than the alkylbenzenes. The differences in substituent effect sensitivity a_1 for various parent compounds can be rationalized by a number of factors, including proximity of substituents to the site of ionization and electronic coupling between the alkyl σ orbitals and the ionized molecular orbital. It should be noted that although the observed substituent effects in alkylferrocenes follow the trend of expected "electron releasing" ability of the substituents, the observed sensitivity of ionization energies to substitution will not necessarily hold for other metallocenes given the change in the valence orbital from which the electron is removed. Furthermore, the electron releasing character of alkyl groups commonly observed for ionization of neutral metallocenes does not necessarily hold in other processes, for example, electron attachment to neutral metal complexes.⁶ In the latter cases, the polarizability of the alkyl group may be dominant and apparent "electron withdrawing" trends are seen,⁴² as observed in, for example, the gas-phase acidities of aliphatic alcohols.⁴³

With respect to the construction of Taft parameter correlations such as those in Figure 4, it is notable that parameters for substituents with low ionization potentials can be derived from the data for ferrocene derivative ionizations. For $\text{R} = \text{CH}_2\text{NMe}_2$, the first ionization of the benzene derivative removes an electron from the nitrogen lone pair orbital and not from the benzene ring, which would be a more endoergic process. However, in the case of $(\text{CpCH}_2\text{NMe}_2)(\text{Cp})\text{Fe}$, the ionization occurs at the same site

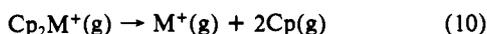
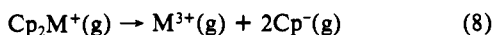
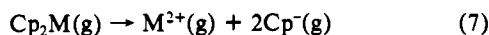
(41) (a) Taft, R. W. In *Steric Effects in Organic Chemistry*; Newman, M. S., Ed.; Wiley-Interscience: New York, 1956. (b) Hansch, C.; Leo, A.; Taft, R. W. *Chem. Rev.* 1991, 91, 165.

(42) (a) Sharpe, P. *Ph.D. Dissertation*; University of Florida: Gainesville, FL, 1990. (b) Richardson, D. E.; Ryan, M. F.; Khan, M. N. I.; Maxwell, K. *J. Am. Chem. Soc.*, submitted for publication.

(43) Brauman, J. I.; Blair, L. K. *J. Am. Chem. Soc.* 1970, 92, 5986.

as in the other alkylferrocenes, thus allowing derivation of a σ_1 parameter for the substituent (-0.049 ± 0.013).

Thermochemical Cycles. Cycles for ionization processes involving metallocenes and their corresponding metal atoms are shown in Figure 5 and are used here to derive average bond disruption enthalpies and solvation energetics in this report. Similar cycles have been used to estimate related thermochemical quantities for a series of coordination complexes and complex ions.¹⁹ In this work, average heterolytic bond disruption enthalpies per bond (half the ΔH° for eqs 7 or 8) will be expressed as $\Delta H_{\text{het}}^\circ$, and the average enthalpy for removal of one Cp ring homolytically (half the ΔH° for eqs 9 or 10) is expressed $\Delta H_{\text{hom}}^\circ$. For the



heterolytic bond cleavages, removal of the first Cp^- ligand should be less endothermic than removal of the second Cp^- ligand due to increased electrostatic attractions between the metal center and Cp^- in the latter case, but only an average of the two disruption enthalpies can be extracted from the cycles used here. Similarly, the first homolytic cleavage of a $\text{M}-\text{Cp}$ bond in a metallocene will not be equivalent to the second. For example, homolytic bond energetics for ferrocene have been studied by pyrolysis techniques, and from the activation barrier for the decomposition of ferrocene to form FeCp , the first bond disruption enthalpy was determined to be 95 kcal mol⁻¹.²⁹ Thus removal of the first Cp ligand homolytically is more endothermic by nearly 30 kcal mol⁻¹ than removal of the second Cp. Once again, however, the applications of the cycles in this work yield only the average of these quantities for the metallocenium ions. Auxiliary data used in the thermochemical calculations are given in Table IV.

In some cases, we have used free energy of ionization data for the metallocenes in bond disruption enthalpy calculations for the metallocenium ions. The validity of combining free energies of ionization of the metallocenes with other enthalpy data is dependent upon the accuracy of using ΔG_i° at 350 K for ΔH_i° at 298 K. This approximation relies on generally small effects of entropy changes on estimated bond enthalpies. As an estimate of the maximum error expected from the approximation, Cp_2Mn is expected to have the largest $|\Delta S_i^\circ|$ of the metallocenes studied in this work. At 350 K, the entropy contribution to the total free energy of ionization for manganocene is 4 kcal mol⁻¹ assuming a large $|\Delta S_i^\circ|$ of 12 cal mol⁻¹ K⁻¹. Even with this relatively large entropy change, the largest error estimated for the case of manganocene is not expected to exceed 2 kcal mol⁻¹ per bond. In general, the assumption that $\Delta G_{i,350}^\circ \approx \Delta H_{i,298}^\circ$ for other metallocenes is adequate since the entropy contribution is expected to be very small with respect to the value for the free energy of ionization. When compared with the values for heterolytic disruption and homolytic disruption of the metallocene cations, the error introduced by the $\Delta G_i^\circ \approx \Delta H_i^\circ$ assumption is small (about 1–2% of calculated homolytic bond enthalpies). Heat capacity corrections in going from 350 to 298 K are also expected to be small. The heat capacity correction in the case of ferrocene has been estimated from the spectroscopic data used in the entropy calculations, and the estimated change in ΔH_i° values from 350 to 298 K is only 0.1 kcal mol⁻¹.

Heterolytic and Homolytic Bond Enthalpies for Metallocenes and Metallocenium Ions. The thermochemical bond enthalpy data derived from energy cycles are presented in Table V. The estimated errors reported for homolytic and heterolytic enthalpies take into account the errors in neutral heats of formation¹³ and estimated errors for the thermal ionization energetics. Bond disruption enthalpies for ruthenocenium, osmocenium, and the substituted ferrocenium ions are not reported due to the lack of reliable values for ΔH_i° of the neutral organometallic compounds and accurate ΔH_i° values for substituted cyclopentadienyl compounds.

Table V. Mean Bond Disruption Enthalpies for Some Metallocenes^a

Cp_2M	$\Delta H_{\text{het}}^\circ$ [$\text{M}^{2+}-\text{Cp}^-$]	$\Delta H_{\text{het}}^\circ$ [$\text{M}^{3+}-\text{Cp}^-$]	$\Delta H_{\text{hom}}^\circ$ [$\text{M}-\text{Cp}^\cdot$]	$\Delta H_{\text{hom}}^\circ$ [$\text{M}^+-\text{Cp}^\cdot$]
V	303 ± 3	563 ± 4	95 ± 2	95 ± 3
Mn	286 ± 3	604 ± 5	59 ± 2	74 ± 4
Fe	318 ± 3	593 ± 4	79 ± 1	91 ± 3
Ni	326 ± 3	649 ± 4	67 ± 2	83 ± 3

^a Units are kcal mol⁻¹.

A point to be made in examining the data in Table V is that the homolytic bond enthalpies are larger for the ions than for the neutrals with the exception of vanadocene. The bond enthalpy difference between the ion and the neutral is thermochemically dependent on the enthalpies of ionization of the compound and the metal atom (see Figure 5). For example, the difference for $\Delta H_{\text{hom}}^\circ$ between ferrocene and ferrocenium is relatively large because the first ΔH_i° of the iron atom⁴⁴ is larger than the ΔH_i° of ferrocene. The ionization enthalpy of $\text{V}(\text{g})$ ⁴⁴ is equal to $\Delta H_i^\circ(\text{Cp}_2\text{V})$, therefore the vanadocenium ion homolytic bond enthalpy, $\Delta H_{\text{hom}}^\circ(\text{Cp}_2\text{V}^+)$, is essentially the same as $\Delta H_{\text{hom}}^\circ(\text{Cp}_2\text{V})$. It is important to recognize that bond disruption enthalpy values depend on the initial and final states in the process, thus interpretation of changes in trends for different metal compounds cannot be based on the nature of the metallocene itself but must also include the state of the metal atom or ion that results from bond disruption.

As expected, the magnitude of the $\Delta H_{\text{het}}^\circ$ values for the metal complexes is larger than corresponding $\Delta H_{\text{hom}}^\circ$ values. On comparison of the metallocenes and metallocenium ions, it is seen that the $\Delta H_{\text{het}}^\circ$ values for the ions are approximately twice those estimated for the neutrals. This is a common ratio found for other heterolytic bond disruptions involving M^{2+} versus M^{3+} ions (e.g., in metal acetylacetonate complexes¹⁹ and metal ion hydration energies⁴⁵).

Differential Solvation Free Energies for Metallocene Redox Couples. Derived differential solvation free energies, $\Delta\Delta G_{\text{sol}}^\circ$, are determined by combining solution $E_{1/2}$ data⁴⁶ at 298 K with ΔG_i° at 350 K. Because of the relatively small effect of the entropy term for these couples, estimates of $\Delta G_{i,298}^\circ$ from 350 K data will lead to only small errors (less than 1 kcal mol⁻¹). Values of $E_{1/2}$ are used to make estimates of $\Delta G_i^\circ(\text{Cp}_2\text{M})(\text{soln})$, and from Figure 5, the $\Delta\Delta G_{\text{sol}}^\circ$ values for metallocene redox couples are derived from the lower thermochemical cycle. In the sign convention used here, a negative value of $\Delta\Delta G_{\text{sol}}^\circ$ represents decreased exoergicity for the reduction of a metallocenium ion in solution compared to the gas phase. An analysis of the estimation of absolute electrode potentials for redox couples in solution has been given earlier,⁹ and a similar approach has been used for derivation of $\Delta\Delta G_{\text{sol}}^\circ$ quantities in this work. Specifically, a value of 4.44 V has been used for the absolute potential of the standard hydrogen electrode and no corrections for liquid junction potentials have been applied to the $E_{1/2}$ data for the metallocenes.⁹ In addition, the stationary electron convention is used for both the gas-phase and solution thermochemistry, although at 298 K the thermal electron convention fortuitously yields identical results for ΔG_i° values.⁴²

The electrochemical $E_{1/2}$ values used in the estimates of $\Delta\Delta G_{\text{sol}}^\circ$ values are shown in Table VI. Most of the values were obtained from a single literature source and were measured under common experimental conditions.⁴⁶ The solvent is acetonitrile for all quoted $E_{1/2}$ values except for vanadocene (THF)^{46a} and ruthenocene (CH_2Cl_2).^{46b} Table VI presents the derived differential solvation energies for the metallocenes and the corresponding solution free energies of oxidation for comparison to the gas-phase

(44) (a) Moore, C. E. *Analysis of Optical Spectra*, NSRDS-NBS 34, Office of Standard Reference Data, National Bureau of Standards, Washington, DC. (b) Lide, D. R. *Handbook of Chemistry and Physics*; CRC Press: Boca Raton, 1990.

(45) Rosseinsky, D. R. *Chem. Rev.* 1965, 65, 467.

(46) (a) Holloway, J. D. L.; Gieger, W. E. *J. Am. Chem. Soc.* 1979, 101, 2038. (b) Gassman, P. G.; Winter, C. H. *J. Am. Chem. Soc.* 1988, 110, 6130. (c) Hill, M. G.; Lamanna, W. M.; Mann, K. R. *Inorg. Chem.* 1991, 30, 4687.

Table VI. Electrochemical $E_{1/2}$ Data and Differential Solvation Energies for Some Metallocene $Cp_2M^{+/0}$ Couples

$Cp_2M^{+/0}$	$E_{1/2}^a$ (solvent)	$\Delta G_i^\circ(\text{soln})^b$	$-\Delta\Delta G_{\text{soln}}^\circ$
V	-0.55 ^{c,d} (THF)	95	60
Cr	-0.67 ^c (CH_3CN)	92	39 ^e
Fe	0.31 ^c (CH_3CN)	115	38
Co	-0.94 ^c (CH_3CN)	86	42 ^e
Ni	-0.09 ^c (CH_3CN)	106	38
Ru	1.03 ^f (CH_2Cl_2)	131	33
Os	0.75 ^g (CH_3CN)	125	36
Mn	(-0.13)	(105) ^h	(38) ^h

^a Values reported in volts using 0.1 M Bu_4NPF_6 as supporting electrolyte against SCE, except ruthenocene in 0.1 M Bu_4NTFPB against $Ag/AgCl$ and osmocene in 0.1 M Bu_4NBF_4 against SCE. ^b Units are kcal mol⁻¹. Estimated error limits ± 4 kcal mol⁻¹. ^c See ref 46a. ^d Irreversible. ^e Estimated from vertical ionization energy taken from ref 12a. ^f See ref 46c. ^g Gubin, S. P.; Smirnova, S. A.; Denisovich, L. I.; Lubovich, A. A. *J. Organomet. Chem.* **1971**, *30*, 243. ^h Estimated from data in Figure 6 and reported against SCE.

ionization energies (see Figure 6).

A comparison of $\Delta\Delta G_{\text{soln}}^\circ$ results to values predicted by dielectric continuum theory suggests that the solvation thermochemistry of $Cp_2M^{+/0}$ couples can be adequately modeled by the Born charging model.^{9,45} The Born equation determines the change in electrostatic free energy, $\Delta G_{\text{el}}^\circ$, when a charge on an electrostatic sphere of radius r_{eff} is transferred in a vacuum to a sphere of equivalent volume in a solution of dielectric constant D , and this quantity can be compared directly to $\Delta\Delta G_{\text{soln}}^\circ$.¹⁹

$$\Delta G_{\text{el}}^\circ = (-166z^2/r_{\text{eff}})(1 - 1/D) \text{ kcal mol}^{-1} \quad (11)$$

For eq 11, z denotes the fundamental charge of the ion (here 1+). From crystallographic data,³⁸ the radii for Cp_2Fe and Cp_2Ni are estimated to be 3.9 and 3.7 Å, respectively.^{21b} The r_{eff} obtained from the Born equation for a $\Delta G_{\text{el}}^\circ = -38$ kcal mol⁻¹ in acetonitrile is 4.3 Å. From another point of view, the structural model radius (3.9 Å) predicts a $\Delta\Delta G_{\text{soln}}^\circ$ value of -41 kcal mol⁻¹. This close agreement between the structurally estimated radii and the thermochemical radii is consistent with relatively small specific interactions between solvent and complex as well as the compact structure of metallocenes. The same conclusion was obtained for $Cp_2Fe^{+/0}$ by Krishtalik et al.,⁴⁷ who used a value for the free energy of ionization of ferrocene based on photoelectron data. For comparison, in the tris(acetylacetonate) metal complexes,³⁴ where polar solvent molecules can interpenetrate between the chelating bidentate ligands, the experimental solvation energy is approximately twice the value predicted from the structural model.

Equation 11 predicts that $|\Delta\Delta G_{\text{soln}}^\circ|$ will be reduced by ~ 3 kcal mol⁻¹ for $r_{\text{eff}} = 3.9$ Å when acetonitrile ($D = 36$) is replaced by CH_2Cl_2 ($D = 9$). From the reversible potentials for $Cp_2M^{+/0}$ ($M = Fe, Ru, Os$) in CH_2Cl_2 given by Hill et al.,^{46c} lower but essentially equal $\Delta\Delta G_{\text{soln}}^\circ$ values (-34 ± 1 kcal mol⁻¹) are estimated for all three couples.

The exception to the observed trend in differential solvation energies is noted for Cp_2V oxidation, which has a $\Delta\Delta G_{\text{soln}}^\circ$ value more negative by ~ 20 kcal mol⁻¹. This additional stabilization of the cation can be attributed to inner sphere coordination of solvent following oxidation.^{46a} Figure 6 demonstrates the periodic trends for $\Delta G_i^\circ(Cp_2M)$ in solution and the gas phase. From the trends in Figure 6, a prediction can be made for the unknown $E_{1/2}$ for Cp_2Mn , -0.13 V versus SCE.

Conclusions

Free energies of ionization have been determined for a number of gas-phase metallocenes. These ETE data complement and extend information on the oxidation energies of metallocenes obtained previously by photoelectron spectroscopy and electrochemistry. Temperature-dependent ETE studies on selected equilibria have established experimental enthalpy and entropy of ionization values for ferrocene. Although the present data are

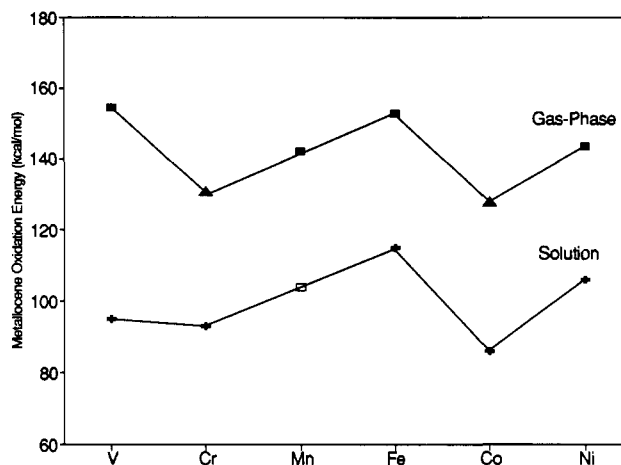


Figure 6. Plot demonstrating the periodic trend of ionization energies for first transition row metallocenes. Gas-phase data include ΔG_i° values derived in this work (filled squares) and vertical ionization energies (triangles). Solution (acetonitrile except Cp_2V in THF) oxidation energies were determined through thermochemical cycles. An estimate of the $\Delta G_i^\circ(\text{soln})$ for manganocene (versus SCE) is included.

consistent with a relatively large value of $\Delta S_i^\circ(Cp_2Fe)$, statistical mechanical analysis and previous PHPMS results suggest that a smaller ΔS_i° (~ 5 cal mol⁻¹ K⁻¹) is appropriate. The positive entropy change for ferrocene ionization can be attributed to roughly equal contributions from intramolecular vibrational degrees of freedom and changes in electronic entropy. Comparison of ETE data with PES spectra for Cp_2V and Cp_2Os yields the same values for adiabatic ionization potentials within experimental error.

The ETE results have been incorporated into thermochemical cycles to allow estimations of bond disruption enthalpies for certain gas-phase metalocenium ions as well as differential solvation energies for several $Cp_2M^{+/0}$ couples. Solvation of a gas-phase metallocene decreases the ionization energy by a relatively constant amount (~ 1.6 eV with acetonitrile as solvent). Solvation is therefore secondary to metal ligation in determining the potential of a $Cp_2M^{+/0}$ couple relative to the ionization of the corresponding $M^{2+}(g)$ ion (ligation of M^{2+} by two Cp^- ligands reduces the ionization energy by ca. 13 ± 1 eV).

Experimental Section

Electron-Transfer Equilibrium Studies. Electron-transfer equilibrium studies were performed by using a Nicolet FT/MS 1000 Fourier transform ion cyclotron resonance mass spectrometer as previously described.^{19,28} Briefly, the pressure of each compound was adjusted to establish a workable pressure ratio to allow equilibria to be monitored. The time dependence of parent ions formed from neutral molecules of known partial pressure was monitored as the molecular ions underwent electron transfer with neutrals. Reactions were typically followed to ca. 5 or more seconds. Apparent equilibrium was generally attained in less than two seconds.

Reference compounds were sublimed into the FTICR-MS high-vacuum chamber through a precision leak valve. The vapor pressure of most metallocene samples was sufficient to allow for direct introduction into the high-vacuum chamber through a second leak valve. Ruthenocene, Cp_2Ru , and osmocene, Cp_2Os , were introduced by using a heated solids probe positioned adjacent to the reaction cell. The FTICR-MS reaction cell was typically at 350 K as measured by an Omega RTD thin film detector. Positive ions were produced by electron impact at 9–12 eV with beam times ranging between 5 and 25 ms. Ionization of metallocenes and organics occurs with some fragmentation of the molecular ion (vide infra); other unwanted ions are formed by ion-molecule reactions. Prior to study of electron-transfer reactions, several ion ejections were required in order to select only the parent ions.

Since reactions were followed for at least 5 s, all ions formed as a result of EI were assumed to be effectively thermalized through ion-molecule collisions. At a neutral pressure of 10^{-6} Torr at 350 K, a typical metalocenium ion will undergo ca. 30 collisions s⁻¹,⁴⁸ which is believed

(47) Krishtalik, L. I.; Alpatova, N. M.; Ovsyannikova, E. V. *Electrochim. Acta* **1991**, *36*, 435.

(48) The Langevin collision frequency for bis(η^5 -cyclopentadienyl) metallocenes has been estimated to be 1.0×10^9 cm³ s⁻¹.²⁸

sufficient to remove much of the excess rotational and vibrational energy present due to the ionization process. Approach to equilibrium was followed from endoergic and exoergic directions. Prior to reaction, one of the parent ions was ejected from the reaction cell and the population change of both parent ions was monitored at set time intervals. Equilibrium was deemed to have been achieved when the ratio of the two parent ion populations reached a constant value within experimental error.

Partial pressures of the various neutrals were determined by using an ion gauge calibrated with an MKS baratron capacitance manometer (in the 10^{-5} Torr range) extrapolated to experimental conditions. In order to approach dynamic pressure equilibrium throughout the vacuum chamber, the 300 L s^{-1} pumping speed of the diffusion pump connected to the high-vacuum chamber was reduced to ca. 75 L s^{-1} . Neutral gas pressures were calibrated for all reactants in open (75 L s^{-1}) and closed (no pumping) systems. It has been shown that partial pressure is independent of neutral gas leak rate.⁴⁹ A calibrated ion gauge connected to a Granville-Phillips controller was positioned at the site of the reaction cell with the magnetic field off, thus providing a field free vacuum system. The pressure measured at the middle of the vacuum chamber where the reaction cell is located, was equivalent to metallocene pressures determined at the remote ion gauge following pressure calibrations.⁴⁹

Temperature Dependence. The temperature dependencies of electron-transfer equilibria were investigated by using a customized cell heater designed to heat a $1'' \times 1'' \times 1\frac{3}{4}''$ analyzer cell. The heater consisted of two Macor plates ($1\frac{1}{2}'' \times 2'' \times \frac{1}{4}''$) (Astro Met Inc.) attached to the long sides of the reaction cell. Ni-Cu wire (0.015'' diameter, Omega) was wrapped around the external Macor plates and was resistively heated by using an Omega digital temperature controller (up to temperatures of up to 520 K). Cell temperatures were measured by using an Omega RTD thin film detector fastened to the analyzer cell. Additionally, the entire high-vacuum chamber was heated by using the

vacuum bake-out system in order to minimize radiative temperature loss to the vacuum chamber walls.

Following the measurement of K_{eq} at a set temperature, the cell heater and bake-out were allowed to cool to a lower temperature and the entire system was allowed to equilibrate at the new temperature for 30 min. Experimental reproducibility was then tested by following the temperature dependence of K_{eq} as the reaction cell temperature was increased from 350 to 500 K. Cell temperature was measured before and after each reaction and usually fluctuated ± 2 K during a single experiment. Typically, reactions were repeated three times at a single temperature. Linear regression and statistical analyses of the all measured equilibrium constants provided error limits at the 95% confidence level for reported ΔH_{et}° and ΔS_{et}° values.

Compounds. Metallocenes were purchased through Strem Chemicals except for ferrocene and ruthenocene (Aldrich). No further purification was required except for Cp_2Mn , which was resublimed prior to use. Organic reference compounds were purchased from Aldrich except *N,N*-diethyl-*p*-toluidine (Alfa Chemicals). A sample of 1,1'-bipyridine^{14c} was donated by Professor Stephen Nelsen (U. Wisconsin). Organic reference compounds were used without further purification. Liquid samples were degassed through several freeze-pump-thaw cycles prior to use.

Far-Infrared Spectroscopy. Ferrocene salts in Table II were prepared according to literature procedures.^{22a,32} The samples were prepared as dilute 13-mm polyethylene pellets. Far-infrared spectra were recorded using a Bruker IFS 113 V spectrophotometer in the 50-750 cm^{-1} spectral region.

Acknowledgment. This work was supported by a grant from the National Science Foundation (CHE 9008663). The authors are grateful to Professor Nelsen and Peter A. Petillo for donation of the alkylhydrazine reference compound. The assistance of Professor William Weltner and Dr. San Li with the measurement of far-IR spectra is gratefully acknowledged. Professor M. Weaver kindly brought ref 47 to our attention.

(49) (a) Bruce, J. E.; Ryan, M. F. Unpublished Results. (b) Bruce, J. E.; Eyley, J. R. *J. Am. Soc. Mass Spectrom.*, in press.

Trimethyl Phosphate: The Intrinsic Reactivity of Carbon versus Phosphorus Sites with Anionic Nucleophiles

Rachel C. Lum[†] and Joseph J. Grabowski^{*‡}

Contribution from the Departments of Chemistry, Harvard University, Cambridge, Massachusetts 02138, and University of Pittsburgh, Pittsburgh, Pennsylvania 15260. Received March 13, 1992

Abstract: The thermally equilibrated (298 ± 3 K) gas-phase ion-molecule reactions of trimethyl phosphate with a variety of anions in 0.3 Torr of helium buffer gas have been examined using the flowing afterglow technique. Inorganic anions including amide, hydroxide, alkoxides, and fluoride, as well as the hydrogen sulfide anion, and organic anions including benzenide, allyl, and benzyl anions, as well as the conjugate bases of acetonitrile and acetaldehyde, were used as reactant anions. Two reaction pathways account for essentially all observations: (i) reductive elimination across a carbon-oxygen bond yielding, as the product ion, $(CH_3O)_2PO^-$ and (ii) nucleophilic substitution at carbon yielding, as the product ion, $(CH_3O)_2PO_2^-$. For all anions that displayed bimolecular reaction pathways, products arising from substitution at carbon are found. The strongest bases (e.g., amide and hydroxide) produce reductive elimination products from trimethyl phosphate. In stark contrast to the reactivity of trimethyl phosphate in solution, particularly in water, anion reaction at phosphorus is completely unimportant, being found as a trace product for the oxygen-centered nucleophiles only. The reaction at phosphorus, an S_N2 -type process, cannot compete with the S_N2 reaction at carbon, because the reaction at carbon has a better leaving group. The bracketed gas-phase acidity of dimethyl phosphate is found to be $\Delta H_{acid}^{\circ}[(CH_3O)_2PO_2H] = 332 \pm 4$ kcal mol^{-1} .

Phosphate esters are an integral part of many biologically active molecules ranging from DNA and ATP to pesticides and nerve agents.¹ It follows then that reactions of phosphate esters, typically called phosphate-transfer reactions, play a critical role in

the chemical processes of life. The mechanism by which enzyme-catalyzed phosphate transfers occur has been studied extensively using both enzymatic and model systems in the condensed phase^{2,3} and theoretical modeling in the gas phase;⁴ enzymatic

[†]Harvard University.

[‡]University of Pittsburgh.

(1) Emsley, J.; Hall, D. *The Chemistry of Phosphorus*; John Wiley: New York, 1976; Chapters 11 and 12.